Reciprocal Role of ERK and NF-κB Pathways in Survival and Activation of Osteoclasts

Tsuyoshi Miyazaki,* Hideki Katagiri,‡ Yumi Kanegae,§ Hiroshi Takayanagi,* Yasuhiro Sawada,* Aiichiro Yamamoto,* Mattew P. Pando,‖ Tomoichiro Asano,‡ Inder M. Verma,‖ Hiromi Oda,* Kozo Nakamura,* and Sakae Tanaka*

*Department of Orthopaedic Surgery and ‡Third Department of Internal Medicine, Faculty of Medicine, The University of Tokyo, Bunkyo-ku, Tokyo 113-0033, Japan; §Laboratory of Molecular Genetics, Institute of Medical Science, The University of Tokyo, Minato-ku, Tokyo 108-8639, Japan; and ‖Laboratory of Genetics, The Salk Institute for Biological Studies, La Jolla, California 92037

Abstract. To examine the role of mitogen-activated protein kinase and nuclear factor kappa B (NF-κB) pathways on osteoclast survival and activation, we constructed adenovirus vectors carrying various mutants of signaling molecules: dominant negative Ras (Ras^{DN}), constitutively active MEK1 (MEK^{CA}), dominant negative IκB kinase 2 (IKK^{DN}), and constitutively active IKK2 (IKK^{CA}). Inhibiting ERK activity by Ras^{DN} overexpression rapidly induced the apoptosis of osteoclast-like cells (OCLs) formed in vitro, whereas ERK activation after the introduction of MEK^{CA} remarkably lengthened their survival by preventing spontaneous apoptosis. Neither inhibition nor activation of ERK affected the bone-resorbing activity of OCLs. Inhibition of NF-κB pathway with IKK^{DN} virus suppressed the pit-forming activity of OCLs and NF-κB activation by IKK^{CA} expression upregulated it without affecting their survival. Interleukin 1α (IL-1α) strongly induced ERK activation as well as NF-κB activation. Ras^{DN} virus partially inhibited ERK activation, and OCL survival promoted by IL-1α. Inhibiting NF-κB activation by IKK^{DN} virus significantly suppressed the pit-forming activity enhanced by IL-1α. These results indicate that ERK and NF-κB regulate different aspects of osteoclast activation: ERK is responsible for osteoclast survival, whereas NF-κB regulates osteoclast activation for bone resorption.

Key words: osteoclast • adenovirus • apoptosis • Ras • NF-κB

Introduction

Osteoclasts, multinucleated giant cells responsible for bone resorption, are terminally differentiated cells with a short life span. Recent findings suggest that the survival of osteoclasts is precisely regulated through interactions with supporting cells as well as by the action of several cytokines (Fuller et al., 1993; Jimi et al., 1995; Hughes et al., 1996; Selander et al., 1996; Kameda et al., 1997). However, the detailed molecular events implicated in these processes still remain elusive.

The small GTP-binding protein Ras is ubiquitously found in eukaryotic organisms and functions as an inducer of various intracellular signaling pathways including cell proliferation and differentiation (Bourne et al., 1990; Bollag and McCormick, 1991; Kaziro et al., 1991). This cascade can be activated by a variety of receptors (Chambard et al., 1987; L'Allemain et al., 1991; Ahn et al., 1992) and leads to activation of mitogen-activated protein kinase (MAPK)[1] cascades. Upon stimulation, Ras assumes its active GTP-bound form, and recruits the protein kinase Raf-1 to the plasma membrane, where the kinase can be activated (Leevers et al., 1994; Stokoe et al., 1994). Raf-1 stimulates MAP kinase kinases (MEK1 and MEK2), which in turn activate ERK1 (p44MAPK) and ERK2 (p42MAPK) (Kyriakis et al., 1992). Although the Ras/ERK pathway is reported to be an important component of cell survival sig-

Address correspondence to Sakae Tanaka, Department of Orthopaedic Surgery, Faculty of Medicine, The University of Tokyo, 7-3-1 Hongo, Bunkyo-ku, Tokyo 113-0033, Japan. Tel.: 81-3-3815-5411 ext 3375. Fax: 81-3-3818-4082. E-mail: tanakas-ort@h.u-tokyo.ac.jp

[1]*Abbreviations used in this paper:* α-MEM, α-modified minimum essential medium; CSF, colony stimulating factor; EMSA, electrophoretic mobility shift assay; ERK, extracellular signal-regulated kinase; IKK, IκB kinase; IL-1α, interleukin 1α; MAPK, mitogen-activated protein kinase; MEK, MAPK/ERK kinase; MOI, multiplicity of infection; NF-κB, nuclear factor kappa B; OCLs, osteoclast-like cells; TUNEL, Tdt-mediated dUTP dioxigenin nick-end labeling.

nal in hematopoietic cells (Kinoshita et al., 1997), its exact role in osteoclasts has not been characterized.

Nuclear factor kappa B (NF-κB) is a transcription factor that regulates the expression of many genes involved in immune and inflammatory responses (Siebenlist et al., 1994; Baldwin, 1996). Activation of NF-κB is controlled by sequential phosphorylation, ubiquitination, and degradation of its inhibitory subunit, IκB. A large multiprotein complex, the IκB kinase (IKK) signalsome, was found to contain a cytokine-inducible IκB kinase activity that phosphorylates IκB-α and IκB-β. The functional IKK complex contains IKK1 (IKKα), IKK2 (IKKβ), and IKKγ, and both IKK1 and IKK2 appear to make an essential contribution to IκB phosphorylation. Mercurio et al. (1997) reported that Ser177 and Ser181 to Ala mutant of IKK2 inhibited NF-κB activation induced by TNF-α, whereas Ser177 and Ser181 to Glu mutant induced constitutive activation of NF-κB. It was recently reported that mice deficient in both the p50 and p52 subunits of NF-κB fail to generate mature osteoclasts and exhibit severe osteopetrosis (Franzoso et al., 1997; Iotsova et al., 1997). Jimi et al. (1998) also reported the involvement of NF-κB pathways in the survival of osteoclasts promoted by interleukin 1 (IL-1). These results suggest that the NF-κB pathway is important for both the differentiation of osteoclast precursors and the survival of mature osteoclasts.

We recently reported that adenoviral vectors are useful for modulating osteoclast function by transducing foreign genes into osteoclasts (Tanaka et al., 1998). Using this system as well as specific inhibitors, we investigated the role of ERK pathways and NF-κB pathways in the survival and activation of osteoclasts, and found that the ERK activation is essential in maintaining osteoclast survival as is the NF-κB pathway for upregulation of bone-resorbing activity of osteoclasts.

Materials and Methods

Animals and Chemicals

Newborn ddY mice and 8-wk-old male ddY mice were purchased from Shizuoka Laboratories Animal Center. α-Modified minimum essential medium (αMEM) and DME were purchased from GIBCO BRL and Life Technologies Inc., and FBS was purchased from Cell Culture Laboratory. Bacterial collagenase and 1α,25-dihydroxyvitamin D_3 ($1\alpha,25(OH)_2D_3$) were purchased from Wako Pure Chemical Co., and dispase from Godo Shusei Co. MEK inhibitor PD98059, anti–phospho-ERK and anti–IκB-α antibodies were purchased from New England Biolabs, Inc., anti–v-src antibody (clone 327) from Oncogene Research Products, anti–Flag antibody from Sigma Chemicals, and anti–NF-κB (p65) antibody from Santa Cruz Biotechnology. Anti–Ras, anti–MEK1, and anti–ERK antibodies were obtained from Transduction Laboratories. Other chemicals and reagents used in this study were of analytical grade.

Cells and Cell Cultures

Mouse primary osteoblastic cells were obtained from 1-d-old ddY mouse calvaria by enzymatic digestion, and bone marrow cells were from tibiae of 8-wk-old male ddY mice (Takahashi et al., 1988). Osteoblastic cells (5×10^5 cells/dish) were cocultured with bone marrow cells (10^7 cells/dish) on 10-cm dishes or collagen gel-coated dishes in the presence of 10 nM $1\alpha,25(OH)_2D_3$ and 1 μM PGE_2 as previously reported (Akatsu et al., 1992). For protein analysis, osteoclast-like cells (OCLs) were purified after a modification of the method originally reported by Tezuka et al. (1992). In brief, the crude osteoclast preparation placed on plastic dishes was washed with αMEM, and treated with 5 ml of αMEM containing 0.1% collagenase and 0.2% dispase for 10 min to remove osteoblastic cells. The purity of OCLs and their precursors was >90% at the final preparation (Tanaka et al., 1995).

Constructs and Gene Transduction

The recombinant adenovirus vector carrying either dominant negative Ras (Ser17 to Asn, $AxRas^{DN}$), constitutively active MEK1 (Ser218 and Ser222 to Glu, $AxMEK^{CA}$), dominant negative IKK2 (also called IKKβ) (Ser177 and Ser181 to Ala, $AxIKK^{DN}$), or constitutively active IKK2 (Ser177 and Ser181 to Glu, $AxIKK^{CA}$) gene under the control of the CAG (cytomegalovirus IE enhancer + chicken β-actin promoter + rabbit β-globin poly $(A)^+$ signal) promoter was constructed by homologous recombination between the expression cosmid cassette and the parental virus genome in 293 cells as described (Niwa et al., 1991; Miyake et al., 1996); the control virus (Ax1w1) was provided by Dr. Izumu Saito (The University of Tokyo, Bunkyo-ku, Tokyo, Japan). Titers of virus stocks were determined by endpoint cytopathic effect assay with the following modifications. 50 μl of DME/10%FBS was dispensed into each well of a 96-well tissue culture plate, and then eight rows of threefold serial dilutions of the virus starting from 10^{-4} dilutions were prepared. 3×10^5 293 cells in 50 μl of DME/10%FBS was added to each well. The plate was incubated at 37°C in 5% CO_2 in air, and 50 μl of DME/10%FBS was added to each well every 3 d. 12 d later, the endpoint of the cytopathic effect was determined by microscopy, and the 50% tissue culture infectious dose ($TCID_{50}$) was calculated. One $TCID_{50}$/ml approximately corresponds to one plaque forming unit (PFU)/ml (Kanegae et al., 1994). The efficiency of infection is affected not only by the concentration of viruses and cells, but also by the ratio of viruses to cells, the multiplicity of infection (MOI). In this study, MOI is expressed as a measure of titer how many PFU are added to every cell. Infection of adenovirus vectors to OCLs was carried out following the method previously described (Tanaka et al., 1998). In short, mouse cocultures on day 4, when OCLs began to appear, were incubated with a small amount of αMEM containing the recombinant adenoviruses for 1 h at 37°C at an indicated MOI. The cells were washed twice with PBS and further incubated with αMEM/10%FBS at 37°C. Experiments were performed 24 h after the infection.

Western Blotting

All extraction procedures were performed at 4°C or on ice. Cells were washed with ice-cold PBS, and then lysed by adding TNE buffer (1% NP-40, 10 mM Tris-HCl, pH 7.8, 150 mM NaCl, 1 mM EDTA, 2 mM Na_3VO_4, 10 mM NaF, and 10 μg/ml aprotinin). The lysates were clarified by centrifugation at 15,000 rpm for 20 min. An equal amount (20 μg) of protein was subjected to 8% SDS-PAGE under a reducing condition, transferred electrophoretically onto a nitrocellulose membrane, and probed sequentially with an appropriate primary antibody followed by secondary antibodies coupled with HRP (Promega Corp.). Immunoreactive proteins were visualized using ECL Western blotting detection reagents (Amersham Co.) following the procedures recommended by the supplier. The blots were stripped by incubating for 20 min in stripping buffer (2% SDS, 100 mM 2-mercaptoethanol, 62.5 mM Tris-HCl, pH 6.7) at 50°C and reprobed by other antibodies.

Immunoprecipitation and In Vitro Kinase Assay

Treated cell cultures were washed twice with ice-cold PBS and lysed in lysis buffer (20 mM Tris-HCl, pH 7.5, 150 mM NaCl, 1% Triton X-100, 12 mM β-glycerophosphate, 5 mM EGTA, 0.5% deoxycholate, 3 mM DTT, 10 mM NaF, 1 mM Na_3VO_4, 2 μM leupeptin, 20 μg/ml aprotinin, and 1 mM PMSF). After 30 min on ice, cell lysates were cleared by centrifugation at 12,000 *g* for 20 min. The protein concentration in each sample was quantified by the Bradford method, and immunoprecipitation was performed by incubating 200 μl of lysate with 2 μg of anti–ERK2 (p42) antibody (Santa Cruz Biotechnology) for 1 h, and then adding 20 μl of protein A–agarose. After incubation for 1 h at 4°C with end-over-end mixing, the immunocomplex was recovered by centrifugation and washed with washing buffer (20 mM Tris-HCl, pH 7.5, 150 mM NaCl, 5 mM EGTA, 2 mM DTT, and 1 mM PMSF) twice. Kinase activity was assayed for 20 min at 37°C in the presence of 6 μg substrate (MBP), 30 μM ATP, and 20 μCi γ-[^{32}P] ATP in 55 μl assay buffer (20 mM Tris-HCl, pH 7.5, and 20 mM $MgCl_2$). After completion of kinase assays, the protein was resolved by SDS-PAGE, and the gels were dried and subjected to autoradiography. The relative activity of ERK2 was quantified by measuring the radioactivity of phosphorus-32 incorporated into MBP.

DNA Extraction and Electrophoretic Analysis

DNA was prepared and analyzed by gel electrophoresis according to the method described previously (Jimi et al., 1998). In brief, purified OCLs were lysed by incubating at 60°C overnight in a digestion buffer containing 150 mM NaCl, 25 mM EDTA, 100 μg/ml proteinase K, and 0.2% SDS. The DNA was extracted twice with phenol/chloroform/isoamylalcohol and once with chloroform, and precipitated in ethanol with 150 mM CH_3COONa, pH 5.2. The DNA was dissolved in TE buffer (10 mM Tris-HCl, pH 8.0, and 1 mM EDTA) and treated with 20 μg/ml RNase A. The procedure for DNA extraction and precipitation were repeated. 2 μg of DNA was separated by electrophoresis on a 1.5% agarose gel and visualized by ethidium bromide staining with UV light illumination.

TUNEL Assay

Cells undergoing apoptosis were identified by means of the TdT-mediated dUTP-dioxigenin nick-end labeling (TUNEL) method, which specifically labels the 3′-hydroxyl terminal of DNA strand breaks. For the TUNEL procedure, all agents, including buffers, were part of a kit (apoptosis in situ detection kit; Wako Pure Chemical Co.); the staining procedure was carried out according to the manufacturer's recommendation. Negative controls included omission of TdT. Positive controls included treatment of the samples with DNase I. Apoptotic cells were recognized by their dark nuclear staining (TUNEL-positive), and nuclei of nonapoptotic cells were visualized by staining with methyl green.

Survival of OCLs

The survival rate was measured as reported (Jimi et al., 1998). OCLs were purified 24 h after the infection and some of the cultures were subjected to tartrate-resistant acid phosphatase (TRAP) staining. Cell viability/survival is expressed as morphologically intact TRAP-positive multinucleated cells. Other cultures were further incubated for the indicated times, and then the number of living OCLs was counted. The number of viable cells remaining at the different time points is shown as a percentage of the cells at time zero.

Immunofluorescence Microscopy

For immunofluorescence analysis, cells were plated on sterile FBS-coated glass coverslips and purified by treatment with αMEM containing 0.1% collagenase and 0.2% dispase. After purification, OCLs were preincubated for 20 min at 37°C in αMEM without FBS and further incubated in αMEM with IL-1α (10 ng/ml) for indicated times, fixed in PBS containing 4% paraformaldehyde for 15 min, permeabilized with 0.2% Triton X-100 in PBS for 5 min, and then blocked with 5% skim milk in PBS for 20 min at room temperature. Cells were sequentially stained with anti–p65 antibody followed by Cy5-conjugated anti-rabbit IgG (Amersham Co.) as previously reported (Isshiki et al., 1998). The subcellular localization of Cy5-labeled p65 was analyzed by a cooled CCD camera (Roper Scientific).

Electrophoretic Mobility Shift Assay

Nuclear extracts were prepared as described previously (Jimi et al., 1998). For samples of purified OCLs, cells were scraped off each dish and put in ice-cold PBS. The cells were washed in ice-cold PBS, lysed for 10 min in ice-cold hypotonic buffer (buffer A: 10 mM Hepes, pH 7.9, 1.5 mM $MgCl_2$, 10 mM KCl, 0.5 mM DTT, and 0.5 mM PMSF), and lysed for 10 min on ice in buffer A containing 0.1% NP-40. The lysates were centrifuged for 20 s at 12,000 *g*. The pelleted nuclei were resuspended in a high salt lysis buffer (20 mM Hepes, pH 7.9, 420 mM NaCl, 25% glycerol, 1.5 mM $MgCl_2$, 0.2 mM EDTA, 0.5 mM PMSF, and 0.5 mM DTT), incubated at 4°C for 20 min, supplemented with 5 vol of storage buffer (20 mM Hepes, pH 7.9, 100 mM KCl, 20% glycerol, 0.2 mM EDTA, 0.5 mM PMSF, and 0.5 mM DTT), and vortexed for 10 s. Lysed nuclei were centrifuged for 10 min at 12,000 *g*, and the resulting supernatants were referred to as nuclear extracts. Oligonucleotide probes containing consensus sequences for NF-κB was provided by Dr. Jun-Ichiro Inoue (The Institute of Medical Science, The University of Tokyo, Minato-ku, Tokyo, Japan). The DNA binding reaction was performed at room temperature in a volume of 20 μl, which contained the binding buffer (25 mM Tris-HCl, pH 7.5, 1.5 mM EDTA, 7.5% glycerol, 75 mM NaCl, 1.5 mM DTT, 0.3% NP-40, and 1 mg/ml BSA), 1 μg of poly (dI-dC), 10^5 cpm of ^{32}P-labeled probe, and 8 μg of nuclear proteins. After incubation for 30 min, the samples were fractionated on a 4% polyacrylamide gel and visualized by exposing dried gel to film.

Pit Formation Assay

Functionally active OCLs formed in cocultures were obtained by a collagen gel culture system as described by Akatsu et al. (1992). In brief, primary osteoblastic cells and bone marrow cells were cocultured in the presence of 10 nM $1\alpha,25(OH)_2D_3$ and 1 μM PGE_2 on culture dishes (6 cm) coated with 0.2% collagen gel matrix. OCLs 24 h after the infection were recovered by digesting the collagen gel with 0.2% collagenase for 20 min at 37°C. The cells released from the dishes were collected by centrifugation at 250 *g* for 5 min and resuspended in 5 ml of αMEM containing 10% FBS. An aliquot of the crude OCL preparation was transferred onto dentine slices and cultured for an additional 12 h. After 12 h of incubation, the medium was removed and 1 M NH_4OH was added to the wells for 30 min. Adherent cells were removed from the dentine slices by ultrasonication, and the resorption pits were visualized by staining with 1% toluidine blue. The resorbed area was measured using an image analysis system (SYSTEM SUPPLY) linked to a light microscope (Nikon).

Statistical Analysis

Each series of experiments was repeated at least three times. The results obtained from a typical experiment were expressed as the means ± SD. Significant differences were determined using factorial analysis of variance (ANOVA).

Results

Downregulation of Ras Inhibits Osteoclast Survival

Recently, we have reported that a replication-deficient adenovirus vector that contains a reporter gene encoding β-galactosidase efficiently infected human OCLs derived from human giant cell tumors and mouse OCLs formed in vitro (Tanaka et al. 1998). The proportion of β-gal–positive OCLs increased in accordance with the number of recombinant adenoviruses inoculated in the culture, and >85% of OCLs became strongly positive for β-gal activity at an MOI of 100, with no obvious morphological change or toxic effects. As shown in Fig. 1 A, the expression of Ras^{DN} was clearly induced in infected OCLs in an MOI-dependent manner. The bottom panel shows that an equal amount of protein was applied in each lane as determined by the Western blotting of c-Src. We next examined the effect of Ras^{DN} expression on the survival of OCLs. After the treatment with 0.1% collagenase and 0.2% dispase to remove osteoblastic cells, noninfected OCLs and OCLs infected with Ax1w1 or $AxRas^{DN}$ at an MOI of 100 were further incubated in αMEM containing 10% FBS to determine their survival. After the removal of osteoblastic cells, ~70% of OCLs infected with or without Ax1w1 died within 18 h (Fig. 1, D and E). In contrast, almost all the Ras^{DN}-expressed OCLs disappeared within 18 h (Fig. 1, D and E), indicating a critical role of Ras in the survival of osteoclasts.

The Deteriorative Effect of Ras^{DN} Overexpression Is Reversed by $AxMEK^{CA}$ Infection

We next examined the signaling pathways working downstream of Ras in osteoclasts. As shown in the top and middle panels of Fig. 1 C, overexpression of Ras^{DN} clearly inhibited the basal activity of ERK in OCLs and ERK activity was ~90% downregulated in Ras^{DN}-expressed OCLs at an MOI of 100. To determine whether or not

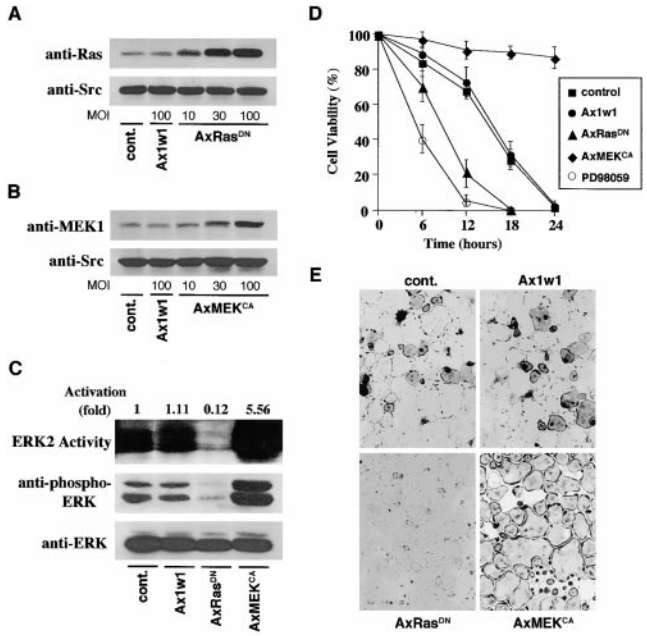

Figure 1. Adenovirus vector-induced Ras^{DN} or MEK^{CA} expression in OCLs. OCLs formed on culture dishes were noninfected or infected with Ax1w1, $AxRas^{DN}$, or $AxMEK^{CA}$ at indicated MOIs. MOI is a measure of titer, meaning how many viruses are infected a cell. After 24 h of infection, OCLs were purified by enzymatic digestion and lysed with TNE buffer. The expression of Ras^{DN} (A) or MEK^{CA} (B) increased in proportion to the MOI of the recombinant adenovirus, whereas the level of c-Src was not significantly changed upon Ras^{DN} or MEK^{CA} induction. (C) Modulation of ERK activity by adenovirus vector–induced Ras^{DN} or MEK^{CA}. OCLs formed on culture dishes were noninfected or infected with Ax1w1, $AxRas^{DN}$, or $AxMEK^{CA}$ at an MOI of 100, and then immunoblotted with anti–phospho-ERK antibody (middle). The stripped membrane was reprobed with anti–ERK antibody (bottom). ERK enzymatic activity was determined by immunocomplex kinase assay with MBP as a substrate (top). Fold increases in ERK activation are shown above each lane. (D) Time course of the survival of OCLs. After purification, noninfected OCLs or OCLs infected with Ax1w1, $AxRas^{DN}$, or $AxMEK^{CA}$ were incubated with αMEM/10%FBS and noninfected OCLs were incubated in the presence of 40 μM PD98059 for indicated times. The number of viable cells remaining at the different time points is shown as a percentage of the cells at time zero. The cell viability rate of OCLs infected with $AxRas^{DN}$ or treated with PD98059 was significantly lower, and that of $AxMEK^{CA}$-infected OCLs is significantly higher at 12, 18, and 24 h than that of control OCLs at 12 and 18 h time points. E shows typical TRAP stainings of OCLs 18 h after purification by the experiment described in D.

modulating ERK activity could affect the survival of OCLs, we used PD98059, a specific inhibitor of ERK activation that does not affect the activation of other MAPKs (Alessi et al., 1995; Favata et al., 1998). PD98059 treatment severely diminished the survival of OCLs (Fig. 1 D). Conversely, upregulation of ERK activity in OCLs using recombinant adenovirus encoding constitutively active MEK1 ($AxMEK^{CA}$) remarkably enhanced their survival (Fig. 1, B–E).

To examine whether or not ERK is the main signaling pathway working downstream of Ras in osteoclasts, we investigated the survival of OCLs that were coinfected with $AxRas^{DN}$ and $AxMEK^{CA}$. Coinfected OCLs expressed Ras^{DN} and MEK^{CA} at the similar level with the cells infected with either Ras^{DN} or MEK^{CA} (Fig. 2 A), and the deteriorative effect of $AxRas^{DN}$ on OCLs was completely rescued by coinfection with $AxMEK^{CA}$ (Fig. 2 B). Nor did the treatment with PD98059, which suppresses the intrinsic MEK activation, inhibit the survival of MEK^{CA}-expressed OCLs (Fig. 2 B). We also found that the expression of Ras^{DN} did not alter the activity of JNK/SAPK or p38 in OCLs (data not shown). Taken together, these findings clearly demonstrate that the Ras/ERK pathway is an important component of survival signal in osteoclasts.

Ras^{DN} Expression Causes Apoptosis of Osteoclasts

We next determined if the reduction of OCL survival by expression of Ras^{DN} was due to apoptosis. After purification, uninfected OCLs or OCLs infected with Ax1w1, $AxRas^{DN}$, or $AxMEK^{CA}$ at an MOI of 100 were cultured for 12 or 24 h. The cells were harvested, and genomic DNA was isolated and resolved on 1.5% agarose gel. After 12 h of culturing, DNA fragmentation was hardly detectable in uninfected OCLs or OCLs infected with Ax1w1, whereas OCLs infected with $AxRas^{DN}$ clearly showed DNA fragmentation (Fig. 3 A). This fragmentation was observed even in uninfected OCLs or OCLs infected with Ax1w1 after 24 h of culture, and the expression of MEK^{CA} markedly inhibited the fragmentation (Fig. 3 A). Almost all the nuclei of MEK^{CA}-expressed OCLs, 24 h after the purification, were stained uniformly with Hoechst 33258, which indicates that the cells were alive and the nuclei

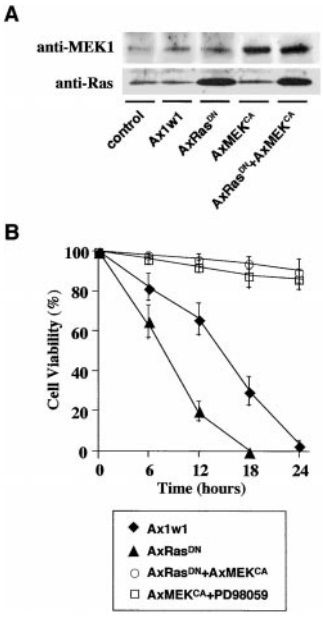

Figure 2. The deteriorative effect of Ras^{DN} overexpression is rescued by $AxMEK^{CA}$ infection. (A) Mouse cocultures on day 4, when OCLs began to appear, were incubated with a small amount of αMEM containing $AxRas^{DN}$ for 1 h at 37°C at an MOI of 100, washed twice with PBS, and incubated with a small amount of αMEM containing $AxMEK^{CA}$ for 1 h at 37°C at an MOI of 100. The cells were washed twice with PBS again and further incubated with αMEM/10%FBS at 37°C. After 24 h of infection, OCLs coinfected with $AxRas^{DN}$ and $AxMEK^{CA}$ were purified by enzymatic digestion and lysed with TNE buffer. Coinfected OCLs expressed Ras^{DN} and MEK^{CA} at the similar level with the cells infected with either $AxRas^{DN}$ or $AxMEK^{CA}$. (B) After purification, OCLs coinfected with $AxRas^{DN}$ and $AxMEK^{CA}$ were incubated with αMEM/10%FBS, and $AxMEK^{CA}$-infected OCLs were incubated in the presence of 40 μM PD98059 for indicated times. The number of viable cells remaining at the different time points is shown as a percentage of the cells at time zero. The toxic effects of Ras^{DN} or PD98059 were entirely reversed by MEK^{CA} expression.

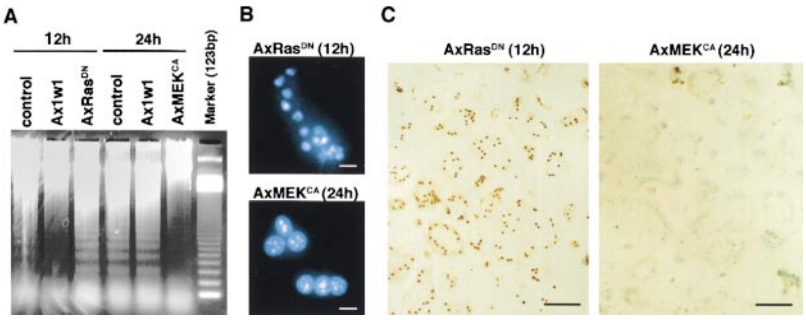

Figure 3. Ras^{DN} expression stimulates apoptosis of OCLs. (A) DNA ladder assay for apoptosis. Fragmentation of DNA in uninfected OCLs and OCLs infected with Ax1w1 was not detectable within 12 h, but it was observed after culturing for 24 h. DNA fragmentation was observed in Ras^{DN}-expressed OCLs within 12 h. In contrast, expression of MEK^{CA} inhibited ladder formation of DNA. The 123-bp ladder DNA was used as a marker. (B) The nuclei of MEK^{CA}-expressed OCLs 24 h after the purification were stained uniformly with Hoechst 33258 (bottom), whereas expression of Ras^{DN} caused fragmentation and condensation of nuclei 12 h after the purification (top). (C) The TUNEL staining of MEK^{CA}- or Ras^{DN}-expressed OCLs was started 24 or 12 h after the purification, respectively. Apoptotic cells were recognized by their dark nuclear staining (TUNEL-positive) and nuclei of nonapoptotic cells were visualized by staining with methyl green. Bars: (B) 10 μm; (C) 100 μm.

were intact, whereas expression of Ras^{DN} caused condensation of >80% of nuclei 12 h after purification (Fig. 3 B). We further determined that ~80% of the nuclei infected with $AxRas^{DN}$ underwent apoptosis 12 h after the purification as shown in Fig. 3 C by TUNEL staining. In contrast, positive TUNEL staining was hardly observed in MEK^{CA}-expressed OCLs even 24 h after the purification (Fig. 3 C). These findings suggest that Ras/ERK pathways contribute greatly to preventing apoptosis of osteoclasts.

IL-1α Activates ERK in OCLs

IL-1α is a proinflammatory cytokine that strongly promotes the survival of osteoclasts by preventing their apoptosis (Jimi et al., 1998). Therefore, we examined the effect of IL-1α treatment on ERK activity in OCLs. After purification, Ax1w1-infected OCLs and Ras^{DN}-expressed OCLs were preincubated for 20 min at 37°C in αMEM without FBS and further incubated in αMEM with IL-1α (10 ng/ml) for various periods. As shown in the top panel of Fig. 4 A,

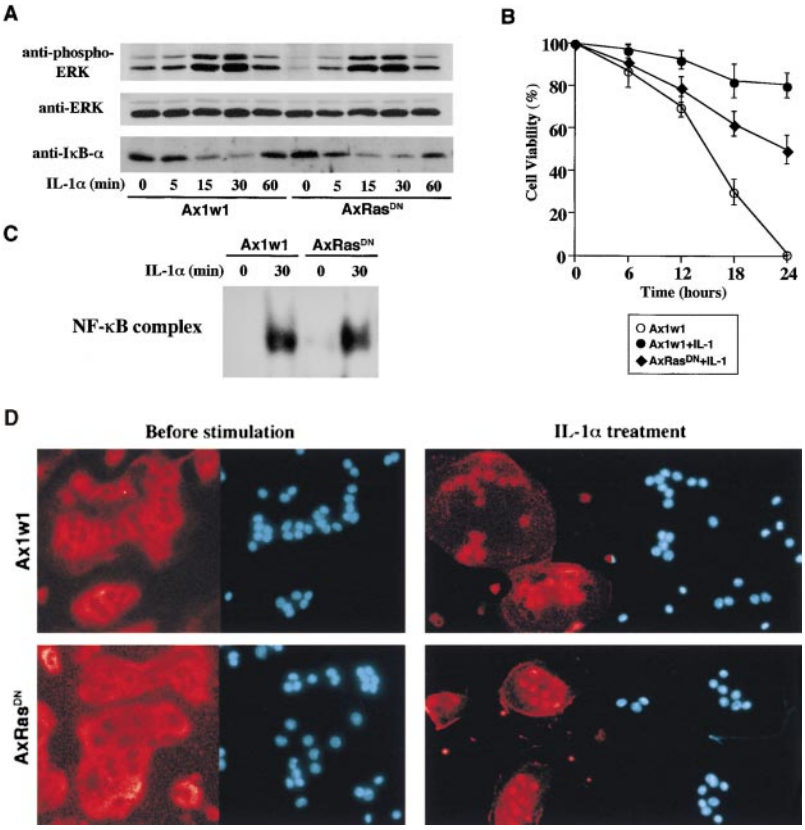

Figure 4. The effects of IL-1α treatment on Ras^{DN}-expressed OCLs. (A, top) Time course of change in ERK activity in Ax1w1- or $AxRas^{DN}$-infected OCLs in response to IL-1α treatment. (middle) Western blot analysis of the expression of ERK protein. (bottom) Time course of change in the protein level of IκB in Ax1w1- or $AxRas^{DN}$-infected OCLs. (B) Effects of $AxRas^{DN}$ on the survival of OCLs promoted by IL-1α. After purification, Ax1w1- or $AxRas^{DN}$-infected OCLs were incubated with αMEM/10%FBS in the presence of IL-1α (10 ng/ml) for indicated times. The number of viable cells remaining at different time points is shown as a percentage of the cells at time zero. $AxRas^{DN}$ partially inhibited the promotion of OCL survival induced by IL-1α. (C) Ax1w1- or $AxRas^{DN}$-infected OCLs were incubated with 10 ng/ml IL-1α for indicated time periods. Equivalent amounts of nuclear extract protein were incubated with a radiolabeled probe containing NF-κB binding site. Activation of NF-κB was determined using EMSA. (D) Purified Ax1w1-infected OCLs or Ras^{DN}-expressed OCLs were treated with IL-1α (10 ng/ml) for 0 or 30 min. Cells were fixed and incubated with antibodies against p65 followed by Cy5-conjugated anti–rabbit immunoglobulins. The subcellular localization of Cy5-labeled p65 (red) was observed by a cooled CCD camera. To visualize the nuclei of the OCLs, the cells were further stained with Hoechst 33258 (blue). Before stimulation, p65 was localized in the cytoplasm, especially around the nuclei of OCLs infected with Ax1w1 or $AxRas^{DN}$. At 30 min, p65 was detected in most of the nuclei of Ax1w1- or $AxRas^{DN}$-infected OCLs in response to IL-1α.

IL-1α stimulated a rapid and transient increase in ERK activity in OCLs. ERK activation in response to IL-1α was transient, reaching the highest level after 15–30 min of stimulation and returning to the basal level after 60 min. Stimulation of ERK activity was not accompanied by a change in the expression level of ERK protein (Fig. 4 A, middle). As previously reported by Jimi et al. (1998), IL-1α treatment strongly promoted the survival of OCLs (Fig. 4 B). Interestingly, the expression of Ras^{DN} in OCLs only partially inhibited the ERK stimulation induced by IL-1α, as shown in the top panel of Fig. 4 A, and partially suppressed the promotion of their survival induced by IL-1α (Fig. 4 B).

Ras^{DN} Expression Does Not Affect the IL-1α–induced Nuclear Translocation of NF-κB in OCLs

Because activation of NF-κB was reported to be involved in the survival of osteoclasts promoted by IL-1α (Jimi et al., 1998), we examined the effect of Ras^{DN} protein on the activation of NF-κB in response to IL-1α. NF-κB is present in the cytosol in an inactive state, complexed with the inhibitory IκB proteins. Activation occurs via phosphorylation of IκB-α at Ser 32 and 36, which promotes the degradation of IκB-α, resulting in the dissociation and nuclear translocation of active NF-κB (Traenckner et al., 1995; Chen et al., 1996). As shown in the bottom panel of Fig. 4 A by Western blotting, IκB-α expression rapidly decreased upon IL-1α stimulation and returned to the basal level after 60 min of stimulation in Ax1w1-infected OCLs. The bottom panel of Fig. 4 A shows that Ras^{DN} expression in OCLs did not affect the kinetics of the degradation of IκB-α by IL-1α. The change in the localization of NF-κB in OCLs treated with IL-1α was also examined immunocytochemically using specific antibodies against the p65 subunit of NF-κB. Before stimulation, p65 was diffusely distributed throughout the cytoplasm. Consistent with the previous report (Jimi et al., 1998), when purified Ax1w1-infected OCLs were treated with IL-1α for 30 min, p65 was detected in most nuclei of the cells. Overexpression of Ras^{DN} did not affect the kinetics of nuclear translocation of NF-κB in OCLs (Fig. 4 D). Consistent with the results of the immunocytochemistry, electrophoretic mobility shift assay (EMSA) showed that NF-κB binding activity was not impaired in Ras^{DN}-overexpressed OCLs (Fig. 4 C).

Modulation of NF-κB Activity Did Not Affect the Survival of OCLs

To further examine the role of NF-κB pathway in osteoclasts, we constructed adenovirus vectors encoding dominant negative IKK2 (IKK^{DN}) and constitutively active IKK2 (IKK^{CA}) with Flag tag, and investigated their effects on OCLs. Fig. 5 A demonstrates the clear induction of IKK^{DN} and IKK^{CA} in infected OCLs in an MOI-dependent manner. Fig. 5 B shows that the degradation of IκB-α induced by IL-1α treatment was strongly blocked by IKK^{DN} expression. Immunocytochemical studies showed that IKK^{DN} expression inhibited nuclear translocation of p65 in IL-1α–stimulated OCLs (Fig. 5 D), and <25% of the nuclei of OCLs were positively stained for p65 even after 30 min of IL-1α stimulation. In contrast, >60% of the nuclei of $AxIkk^{CA}$-infected OCLs were positively stained without any stimulation (Fig. 5 D). EMSA demonstrated that NF-κB activation was inhibited in IKK^{DN}-expressed OCLs treated with IL-1α. Conversely, slight constitutive NF-κB activation was observed in IKK^{CA}-expressed OCLs (Fig. 5 C). As shown in Fig. 6, neither IKK^{DN} nor IKK^{CA} virus infection significantly changed the survival of OCLs with or without IL-1α stimulation.

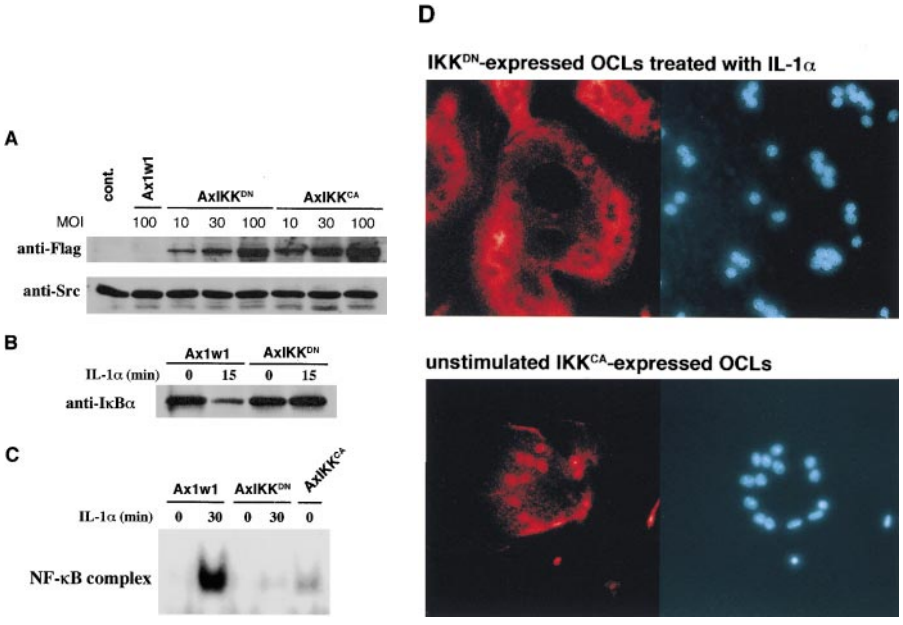

Figure 5. Adenovirus vector-induced IKK^{DN} or IKK^{CA} expression in OCLs. (A) OCLs formed on culture dishes were noninfected or infected with Ax1w1, $AxIKK^{DN}$, or $AxIKK^{CA}$ at indicated MOIs. After 24 h of infection, OCLs were purified by enzymatic digestion and lysed with TNE buffer. The total cell lysate proteins were Western blotted with anti–Flag antibody, which recognizes Flag-tagged exogenous IKK2. The expression of IKK^{DN} or IKK^{CA} increased in proportion to the MOI of the recombinant adenovirus, whereas the level of c-Src was not significantly changed upon IKK^{DN} or IKK^{CA} induction. (B) After purification, Ax1w1- or $AxIKK^{DN}$-infected OCLs were preincubated for 20 min at 37°C in αMEM without FBS and further incubated in αMEM with IL-1α for 15 min. The amount of IκB-α was determined by Western blotting. (C) Ax1w1, $AxIKK^{DN}$, or $AxIKK^{CA}$-infected OCLs were incubated with 10 ng/ml IL-1α for the indicated time periods. Equivalent amounts of nuclear extract protein were incubated with a radiolabeled probe containing NF-κB binding site. Activation of NF-κB was determined using EMSA. (D) Purified IKK^{DN}- or IKK^{CA}-expressed OCLs were treated with IL-1α (10 ng/ml) for 30 or 0 min, respectively. Cells were fixed and incubated with antibodies against p65 followed by Cy5-conjugated anti–rabbit immunoglobulins. IKK^{DN} expression inhibited p65 nuclear translocation in IL-1α–treated OCLs. In contrast, IKK^{CA} induced constitutive nuclear localization of p65 in the absence of cell stimulation.

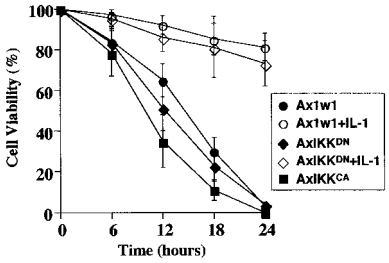

Figure 6. The effect of IKK^{DN} and IKK^{CA} expression on the survival of OCLs. After purification, OCLs infected Ax1w1, Ax-IKK^{DN}, or AxIKK^{CA} were incubated with αMEM/10%FBS and Ax1w1- or AxIKK^{DN}-infected OCLs were incubated in the presence of IL-1α (10 ng/ml) for the indicated times. The number of viable cells remaining at the different time points is shown as a percentage of the cells at time zero.

NF-κB Pathway Is Involved in Osteoclast Activation for Bone Resorption

We next examined the role of ERK pathways and NF-κB pathways on bone-resorbing activity of OCLs using the adenovirus vectors described above. This activity of OCLs was quantified by measuring the pit area formed on dentine slices as previously reported (Tamura et al., 1993). To minimize the influence of the different survival periods on the pit formation by OCLs, we performed the pit assay after 12 h of culturing and the pit-forming activity is expressed as the area resorbed per osteoclast. As shown in Fig. 7 A, neither Ras^{DN} nor MEK^{CA} expression altered the pit-forming activity of OCLs, indicating that the ERK pathway is not involved in the bone-resorbing activity of the individual OCL. In contrast, OCL pit-forming activity was significantly inhibited by induction of IKK^{DN}, whereas overexpression of IKK^{CA} enhanced it. Because IL-1α strongly promotes not only the survival of osteoclasts, but also their bone resorbing activity (Boyce et al., 1989), we examined the effect of IKK^{DN} expression on the bone-resorbing activity promoted by IL-1α. As shown in Fig. 7 B, IL-1α treatment strongly enhanced the OCL pit-forming activity, and inhibiting NF-κB activation by the IKK^{DN} virus significantly suppressed the pit-forming activity enhanced by IL-1α.

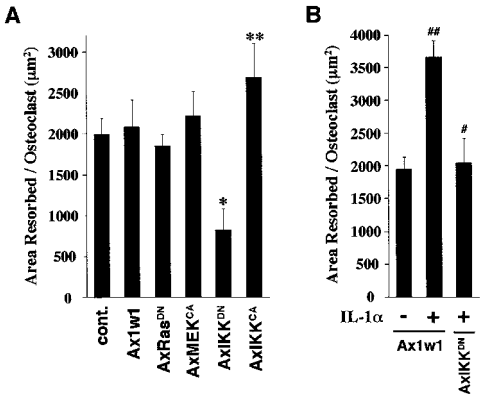

Figure 7. Dentine-resorbing activity of OCLs expressing Ras^{DN}, MEK^{CA}, IKK^{DN}, or IKK^{CA}. (A) OCLs 24 h after the infection were restored by digesting the collagen gel with 0.2% collagenase for 20 min at 37°C and an aliquot of the crude OCL preparation was transferred onto dentine slices (ϕ 5 mm) as well as on 96-well culture plates and further cultured for 12 h. The resorbed area on dentine slices was measured using an image analysis system, and the number of TRAP-positive OCLs on culture plates was counted by light microscopy. The bone-resorbing activity of the cells was expressed as the resorbed area per osteoclast. The values are means ± SD ($n = 8$). (one asterisk) Significantly less than control, $P < 0.05$. (two asterisks) Significantly greater than control, $P < 0.05$. (B) After the transfer onto dentine slices, Ax1w1- or Ax-IKK^{DN}-infected OCLs were further incubated for 12 h in the presence or absence of IL-1α (10 ng/ml). The pit-forming activity of AxIKK^{DN}-infected OCLs treated with IL-1α was significantly lower than that of Ax1w1-infected OCLs treated with IL-1α (#$P < 0.01$). The values are means ± SD ($n = 8$). ##Significantly greater than Ax1w1-infected OCLs without IL-1α stimulation, $P < 0.01$.

Colony-stimulating Factor 1 (CSF-1) Activates ERK, but Not NF-κB in OCLs

Because CSF-1 (also called macrophage colony-stimulating factor) has been reported to prolong the survival of OCLs without upregulating their bone resorbing activity, we examined the effect of CSF-1 treatment on ERK and NF-κB activity in OCLs. As shown in the top panel of Fig. 8 A, ERK activation in response to CSF-1 was transient, reaching the highest level after 2–15 min of stimulation and returning to the basal level after 60 min. Stimulation of ERK activity was not accompanied by a change in the

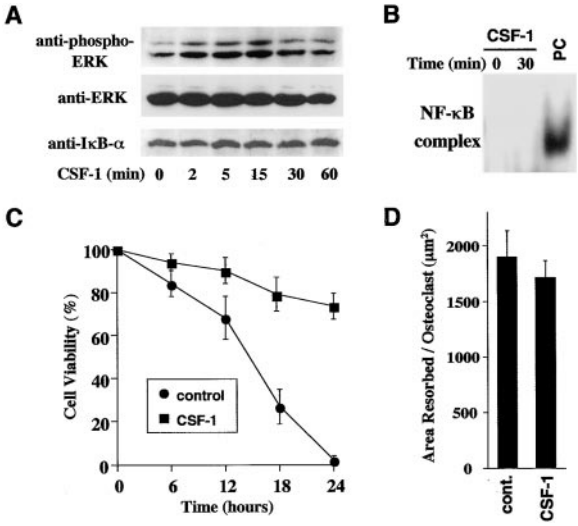

Figure 8. The effects of CSF-1 treatment on OCLs. (A, top) Time course of change in ERK activity in OCLs after stimulation with CSF-1 (100 ng/ml). (middle) Western blot analysis of the expression of ERK protein. (bottom) Time course of change in the protein level of IκB-α in CSF-1–treated OCLs. (B) OCLs were incubated with CSF-1 for indicated time periods. Equivalent amounts of nuclear extract protein were incubated with a radiolabeled probe containing the NF-κB binding site. Activation of NF-κB was determined using EMSA. IL-1α–treated OCLs (right lane) were used as positive controls (PC). (C) After purification, OCLs were incubated with αMEM/10% in the presence or absence of CSF-1 for the indicated times. The number of viable cells remaining at different time points is shown as a percentage of the cells at time zero. (D) After the transfer onto dentine slices, OCLs were further incubated for 12 h in the presence or absence of CSF-1 (100 ng/ml). CSF-1 stimulation did not alter the OCL pit-forming activity. The values are means ± SD ($n = 8$).

expression level of ERK protein (Fig. 8 A, middle). As previously reported (Fuller et al., 1993; Jimi et al., 1995), CSF-1 treatment strongly promoted the survival of OCLs (Fig. 8 C). On the other hand, CSF-1 did not alter the expression level of IκB-α (Fig. 8 A, bottom) and activate NF-κB (Fig. 8 B). In addition, OCL bone-resorbing activity remained unchanged despite CSF-1 stimulation (Fig. 8 D). These results strongly support our findings that ERK and NF-κB pathways are involved in osteoclast survival and activation for bone resorption, respectively.

Discussion

The Ras superfamily of GTPases is implicated in a number of cellular physiological processes including cell proliferation and differentiation, and plays important roles in the organization of cellular architecture and regulation of membrane dynamism in addition to cell cycle control (Bourne et al., 1990; Bollag and McCormick, 1991; Kaziro et al., 1991). Recently, Luckman et al. (1998) reported that the nitrogen-containing bisphosphonates alendronate, ibandronate, and risedronate, which cause apoptosis in osteoclasts and suppress their bone-resorbing activity, inhibit posttranslational modification (prenylation) of proteins with farnesyl or geranylgeranyl isoprenoid groups, including the Ras superfamily of GTPases. Further studies performed by Fisher et al. (1999) demonstrated that alendronate acts directly on osteoclasts and interferes with the generation of geranylgeranyl diphosphate by inhibiting enzymes in the cholesterol biosynthesis pathway, resulting in the suppression of osteoclast function. These findings suggest the critical role of the Ras superfamily in this function.

The pleiotropic functions of the Ras protein are now explained by its capability to activate multiple downstream pathways (Koide et al., 1993; Moodie et al., 1993; Rodriguez-Viciana et al., 1994; Van Aelst et al., 1993, 1994; Vojtek et al., 1993). One of the most important signaling cascades lying downstream of Ras is the MAPK cascade, which is activated via the Ras–Raf interaction. This interaction induces the membrane translocation and activation of Raf, and activated Raf phosphorylates tyrosine/threonine kinase MEK, which in turn phosphorylates ERK. In the present study, we demonstrated the essential role of Ras/ERK pathways in the survival of osteoclasts. First, adenovirus vector carrying a dominant negative mutant of Ras ($AxRas^{DN}$) suppressed ERK activity in OCLs and promoted the apoptosis of OCLs. A similar effect was observed using a MEK inhibitor, PD98059. Second, expression of constitutively active MEK1-induced sustained stimulation of ERK in OCLs and dramatically promoted their survival, and the apoptosis-inducing effect of $AxRas^{DN}$ was completely rescued by coinfection with $AxMEK^{CA}$. Finally, IL-1α, which strongly promotes OCL survival, rapidly stimulates ERK activation in OCLs. It should be noted that overexpression of Ras^{DN} only partially inhibited the ERK activation and suppressed the prolonged survival induced by IL-1α, whereas PD98059 strongly eliminated the effect of IL-1α (data not shown), suggesting that IL-1α stimulates ERK activity via Ras-independent pathways as well. These results clearly demonstrate that ERK activation is indispensable for the survival of osteoclasts, and that Ras is at least partially involved in this process.

It remains elusive how ERK activation stimulates OCL survival. In fibroblasts, ERK activation is followed by phosphorylation of transcription factors and induction of immediate early gene expression. The dimeric transcription factor AP-1 (activator protein-1) is a major target of cell growth, differentiation, and stress signaling pathways (Angel and Karin, 1991; Karin and Hunter, 1995; Whitmarsh and Davis, 1996). AP-1 consists of various combinations of Fos and Jun family members that dimerize via a leucine zipper domain and bind to DNA via an adjacent basic region (Landschulz et al., 1988; Gentz et al., 1989; Kouzarides and Ziff, 1989). The Fos family consists of four gene products (c-Fos, FosB, Fra-1, and Fra-2), whereas the Jun family is made up of three gene products (c-Jun, JunB, and JunD). We also found that sustained stimulation of ERK in OCLs by MEK^{CA} expression as well as IL-1α stimulation increased c-Fos, Fra-2, c-Jun, and JunB expression (data not shown), suggesting that AP-1 activation may be involved in the survival signaling in osteoclasts. Further study will be necessary to elucidate the detail of osteoclast survival signaling.

Jimi et al. (1998) recently reported that the activation of NF-κB is involved in the survival of osteoclasts promoted by IL-1α. They clearly showed the nuclear translocation of NF-κB and degradation of IκB in OCLs in response to IL-1α treatment. The survival of OCLs supported by IL-1α was suppressed by pretreatment with proteasome inhibitors, which inhibits NF-κB activation by preventing IκB degradation, or with antisense oligonucleotides to NF-κB components (Jimi et al., 1998). In contrast to their results, we were unable to show the effect of NF-κB on the survival of OCLs. Consistent with the previous report, IL-1α treatment induced rapid nuclear translocation of NF-κB in OCLs and degradation of IκB. However, overexpression of neither Ras^{DN} nor MEK^{CA} changed the localization of NF-κB in the presence or absence of IL-1α. In addition, either inhibition of NF-κB activity by overexpression of dominant negative IKK (IKK^{DN}) or sustained activation of NF-κB by transducing constitutively active IKK (IKK^{CA}) had little effect on the survival of OCLs with or without IL-1α stimulation. We cannot fully explain the reason for the discrepancy between our results and those of the previous report, but it is possible that proteasome inhibitors and antisense oligonucleotides may possess some undesirable effects on OCLs unrelated to NF-κB inhibition.

However, NF-κB has an important role in the bone-resorbing activity of osteoclasts because adenovirus vector-induced IKK^{DN} expression significantly suppressed the pit-forming activity of OCLs and IKK^{CA} expression enhanced it, although these two viruses had no effect on OCL survival. Members of the TNF receptor family and the IL-1 receptor associated either directly or indirectly with TNF receptor-associated factors (TRAFs), adaptor proteins that recruit and activate downstream signaling transducers (Rothe et al., 1994). TRAF6 is a newly identified member of TRAF, which is not involved in TNF signaling but in IL-1 signaling (Cao et al., 1996; Darnay et al., 1998; Galibert et al., 1998). Not only does TRAF6 activate NF-κB by signaling via NIK and IKK, but it also activates ERK in a Ras-independent manner (Kashiwada et al., 1998). A recent study on TRAF6 knockout mice demon-

strated the essential role of TRAF6 on the activation of osteoclasts (Lomaga et al., 1999). Taken together, it is likely that IL-1α can promote survival and activity of osteoclasts simultaneously via ERK and NF-κB activation, both of which are mediated by TRAF6. Our present study proposes the reciprocal role of ERK and NF-κB pathways in the survival and activation of osteoclasts. Further investigation of these pathways in osteoclasts will give us new insight into the molecular mechanism regulating bone resorption.

R. Yamaguchi (Department of Orthopaedic Surgery, The University of Tokyo) provided expert technical assistance. We thank I. Saito, J. Miyazaki, and J.-I. Inoue (The Institute of Medical Science, The University of Tokyo) for gifts of the recombinant adenovirus vector system, the CAG promoter, and the NF-κB binding oligonucleotide, respectively.

This work was in part supported by a grant from the Japan Orthopaedic and Traumatology Foundation Inc. (No. 0089; Alcare Award) and Grants-in-Aid from the Ministry of Education, Science, Sports and Culture of Japan to S. Tanaka and from Bristol-Myers Squibb/Zimmer Unrestricted Research Grants and Health Science Research Grants from Ministry of Health and Welfare to K. Nakamura.

Submitted: 12 July 1999
Revised: 7 December 1999
Accepted: 7 December 1999

References

Ahn, N.G., D.J. Robbins, J.W. Haycock, R. Seger, M.H. Cobb, and E.G. Krebs. 1992. Identification of an activator of the microtubule-associated protein 2 kinases ERK1 and ERK2 in PC12 cells stimulated with nerve growth factor or bradykinin. *J. Neurochem*. 59:147–156.

Akatsu, T., T. Tamura, N. Takahashi, N. Udagawa, S. Tanaka, T. Sasaki, A. Yamaguchi, N. Nagata, and T. Suda. 1992. Preparation and characterization of a mouse osteoclast-like multinucleated cell population. *J. Bone Miner. Res*. 7:1297–1306.

Alessi, D.R., A. Cuenda, P. Cohen, D.T. Dudley, and A.R. Saltiel. 1995. PD 098059 is a specific inhibitor of the activation of mitogen-activated protein kinase kinase in vitro and in vivo. *J. Biol. Chem*. 270:27489–27494.

Angel, P., and M. Karin. 1991. The role of Jun, Fos and the AP-1 complex in cell-proliferation and transformation. *Biochim. Biophys. Acta*. 1072:129–157.

Baldwin, A.S., Jr. 1996. The NF-κB and IκB proteins: new discoveries and insights. *Annu. Rev. Immunol*. 14:649–683.

Bollag, G., and F. McCormick. 1991. Regulators and effectors of ras proteins. *Annu. Rev. Cell Biol*. 7:601–632.

Bourne, H.R., D.A. Sanders, and F. McCormick. 1990. The GTPase superfamily: a conserved switch for diverse cell functions. *Nature*. 348:125–132.

Boyce, B.F., T.B. Aufdemorte, I.R. Garrett, A.J. Yates, and G.R. Mundy. 1989. Effects of interleukin-1 on bone turnover in normal mice. *Endocrinology*. 125:1142–1150.

Cao, Z., J. Xiong, M. Takeuchi, T. Kurama, and D.V. Goeddel. 1996. TRAF6 is a signal transducer for interleukin-1. *Nature*. 383:443–446.

Chambard, J.C., S. Paris, G. L'Allemain, and J. Pouyssegur. 1987. Two growth factor signalling pathways in fibroblasts distinguished by pertussis toxin. *Nature*. 326:800–803.

Chen, Z.J., L. Parent, and T. Maniatis. 1996. Site-specific phosphorylation of IκBα by a novel ubiquitination-dependent protein kinase activity. *Cell*. 84: 853–862.

Darnay, B.G., V. Haridas, J. Ni, P.A. Moore, and B.B. Aggarwal. 1998. Characterization of the intracellular domain of receptor activator of NF-κB (RANK). Interaction with tumor necrosis factor receptor-associated factors and activation of NF-κB and c-Jun N-terminal kinase. *J. Biol. Chem*. 273: 20551–20555.

Favata, M.F., K.Y. Horiuchi, E.J. Manos, A.J. Daulerio, D.A. Stradley, W.S. Feeser, D.E. Van Dyk, W.J. Pitts, R.A. Earl, F. Hobbs, et al. 1998. Identification of a novel inhibitor of mitogen-activated protein kinase kinase. *J. Biol. Chem*. 273:18623–18632.

Fisher, J.E., M.J. Rogers, J.M. Halasy, S.P. Luckman, D.E. Hughes, P.J. Masarachia, G. Wesolowski, R.G. Russell, G.A. Rodan, and A.A. Reszka. 1999. Alendronate mechanism of action: geranylgeraniol, an intermediate in the mevalonate pathway, prevents inhibition of osteoclast formation, bone resorption, and kinase activation in vitro. *Proc. Natl. Acad. Sci. USA*. 96:133–138.

Franzoso, G., L. Carlson, L. Xing, L. Poljak, E.W. Shores, K.D. Brown, A. Leonardi, T. Tran, B.F. Boyce, and U. Siebenlist. 1997. Requirement for NF-κB in osteoclast and B-cell development. *Genes Dev*. 11:3482–3496.

Fuller, K., J.M. Owens, C.J. Jagger, A. Wilson, R. Moss, and T.J. Chambers. 1993. Macrophage colony-stimulating factor stimulates survival and chemotactic behavior in isolated osteoclasts. *J. Exp. Med*. 178:1733–1744.

Galibert, L., M.E. Tometsko, D.M. Anderson, D. Cosman, and W.C. Dougall. 1998. The involvement of multiple tumor necrosis factor receptor (TNFR)-associated factors in the signaling mechanisms of receptor activator of NF-κB, a member of the TNFR superfamily. *J. Biol. Chem*. 273:34120–34127.

Gentz, R., F.J. Rauscher III, C. Abate, and T. Curran. 1989. Parallel association of Fos and Jun leucine zippers juxtaposes DNA binding domains. *Science*. 243:1695–1699.

Hughes, D.E., A. Dai, J.C. Tiffee, H.H. Li, G.R. Mundy, and B.F. Boyce. 1996. Estrogen promotes apoptosis of murine osteoclasts mediated by TGF-β. *Nat. Med*. 2:1132–1136.

Iotsova, V., J. Caamano, J. Loy, Y. Yoang, A. Lewin, and R. Bravo. 1997. Osteopetrosis in mice lacking NF-κB1 and NF-κB2. *Nat. Med.* 3:1285–1289.

Isshiki, M., J. Ando, R. Korenaga, H. Kogo, T. Fujimoto, T. Fujita, and A. Kamiya. 1998. Endothelial Ca^{2+} waves preferentially originate at specific loci in caveolin-rich cell edges. *Proc. Natl. Acad. Sci. USA*. 95:5009–5014.

Jimi, E., T. Shuto, and T. Koga. 1995. Macrophage colony-stimulating factor and interleukin-1 alpha maintain the survival of osteoclast-like cells. *Endocrinology*. 136:808–811.

Jimi, E., I. Nakamura, T. Ikebe, S. Akiyama, N. Takahashi, and T. Suda. 1998. Activation of NF-κB is involved in the survival of osteoclasts promoted by interleukin-1. *J. Biol. Chem*. 273:8799–8805.

Kameda, T., H. Mano, T. Yuasa, Y. Mori, K. Miyazawa, M. Shiokawa, Y. Nakamaru, E. Hiroi, K. Hiura, A. Kameda, et al. 1997. Estrogen inhibits bone resorption by directly inducing apoptosis of the bone-resorbing osteoclasts. *J. Exp. Med*. 186:489–495.

Kanegae, Y., M. Makimura, and I. Saito. 1994. A simple and efficient method for purification of infectious recombinant adenovirus. *Jpn. J. Med. Sci. Biol*. 47:157–166.

Karin, M., and T. Hunter. 1995. Transcriptional control by protein phosphorylation: signal transmission from the cell surface to the nucleus. *Curr. Biol*. 5:747–757.

Kashiwada, M., Y. Shirakata, J.I. Inoue, H. Nakano, K. Okazaki, K. Okumura, T. Yamamoto, H. Nagaoka, and T. Takemori. 1998. Tumor necrosis factor receptor-associated factor 6 (TRAF6) stimulates extracellular signal–regulated kinase (ERK) activity in CD40 signaling along a Ras-independent pathway. *J. Exp. Med*. 187:237–244.

Kaziro, Y., H. Itoh, T. Kozasa, M. Nakafuku, and T. Satoh. 1991. Structure and function of signal-transducing GTP-binding proteins. *Annu. Rev. Biochem*. 60:349–400.

Kinoshita, T., M. Shirouzu, A. Kamiya, K. Hashimoto, S. Yokoyama, and A. Miyajima. 1997. Raf/MAPK and rapamycin-sensitive pathways mediate the anti-apoptotic function of p21Ras in IL-3-dependent hematopoietic cells. *Oncogene*. 15:619–627.

Koide, H., T. Satoh, M. Nakafuku, and Y. Kaziro. 1993. GTP-dependent association of Raf-1 with Ha-Ras: identification of Raf as a target downstream of Ras in mammalian cells. *Proc. Natl. Acad. Sci. USA*. 90:8683–8686.

Kouzarides, T., and E. Ziff. 1989. Leucine zippers of fos, jun and GCN4 dictate dimerization specificity and thereby control DNA binding. *Nature*. 340:568–571.

Kyriakis, J.M., H. App, X.F. Zhang, P. Banerjee, D.L. Brautigan, U.R. Rapp, and J. Avruch. 1992. Raf-1 activates MAP kinase-kinase. *Nature*. 358:417–421.

L'Allemain, G., J. Pouyssegur, and M.J. Weber. 1991. p42/mitogen-activated protein kinase as a converging target for different growth factor signaling pathways: use of pertussis toxin as a discrimination factor. *Cell Regul*. 2:675–684.

Landschulz, W.H., P.F. Johnson, and S.L. McKnight. 1988. The leucine zipper: a hypothetical structure common to a new class of DNA binding proteins. *Science*. 240:1759–1764.

Leevers, S.J., H.F. Paterson, and C.J. Marshall. 1994. Requirement for Ras in Raf activation is overcome by targeting Raf to the plasma membrane. *Nature*. 369:411–414.

Lomaga, M.A., W.C. Yeh, I. Sarosi, G.S. Duncan, C. Furlonger, A. Ho, S. Morony, C. Capparelli, G. Van, S. Kaufman, et al. 1999. TRAF6 deficiency results in osteopetrosis and defective interleukin-1, CD40, and LPS signaling. *Genes Dev*. 13:1015–1024.

Luckman, S.P., D.E. Hughes, F.P. Coxon, R. Graham, G. Russell, and M.J. Rogers. 1998. Nitrogen-containing bisphosphonates inhibit the mevalonate pathway and prevent post-translational prenylation of GTP-binding proteins, including Ras. *J. Bone Miner Res*. 13:581–589.

Mercurio, F., H. Zhu, B.W. Murray, A. Shevchenko, B.L. Bennett, J. Li, D.B. Young, M. Barbosa, M. Mann, A. Manning, and A. Rao. 1997. IKK-1 and IKK-2: cytokine-activated IκB kinases essential for NF-κB activation. *Science*. 278:860–866.

Miyake, S., M. Makimura, Y. Kanegae, S. Harada, Y. Sato, K. Takamori, C. Tokuda, and I. Saito. 1996. Efficient generation of recombinant adenoviruses using adenovirus DNA-terminal protein complex and a cosmid bearing the full-length virus genome. *Proc. Natl. Acad. Sci. USA*. 93:1320–1324.

Moodie, S.A., B.M. Willumsen, M.J. Weber, and A. Wolfman. 1993. Complexes of Ras. *Proc. Natl. Acad. Sci. USA*. 95:5009–5014.

Niwa, H., K. Yamamura, and J. Miyazaki. 1991. Efficient selection for high-expression transfectants with a novel eukaryotic vector. *Gene*. 108:193–199.

Rodriguez-Viciana, P., P.H. Warne, R. Dhand, B. Vanhaesebroeck, I. Gout, M.J. Fry, M.D. Waterfield, and J. Downward. 1994. Phosphatidylinositol-3-OH kinase as a direct target of Ras. *Nature*. 370:527–532.

Rothe, M., S.C. Wong, W.J. Henzel, and D.V. Goeddel. 1994. A novel family of putative signal transducers associated with the cytoplasmic domain of the 75

kDa tumor necrosis factor receptor. *Cell*. 78:681–692.
Selander, K.S., P.L. Harkonen, E. Valve, J. Monkkonen, R. Hannuniemi, and H.K. Vaananen. 1996. Calcitonin promotes osteoclast survival in vitro. *Mol. Cell. Endocrinol*. 122:119–129.
Siebenlist, U., G. Franzoso, and K. Brown. 1994. Structure, regulation and function of NF-kappa B. *Annu. Rev. Cell Biol*. 10:405–455.
Stokoe, D., S.G. Macdonald, K. Cadwallader, M. Symons, and J.F. Hancock. 1994. Activation of Raf as a result of recruitment to the plasma membrane. *Science*. 264:1463–1467.
Takahashi, N., T. Akatsu, N. Udagawa, T. Sasaki, A. Yamaguchi, J.M. Moseley, T.J. Martin, and T. Suda. 1988. Osteoblastic cells are involved in osteoclast formation. *Endocrinology*. 123:2600–2602.
Tamura, T., N. Takahashi, T. Akatsu, T. Sasaki, N. Udagawa, S. Tanaka, and T. Suda. 1993. New resorption assay with mouse osteoclast-like multinucleated cells formed in vitro. *J. Bone Miner Res*. 8:953–960.
Tanaka, S., N. Takahashi, N. Udagawa, H. Murakami, I. Nakamura, T. Kurokawa, and T. Suda. 1995. Possible involvement of focal adhesion kinase, $p125^{FAK}$, in osteoclastic bone resorption. *J. Cell Biochem*. 58:424–435.
Tanaka, S., T. Takahashi, H. Takayanagi, T. Miyazaki, H. Oda, K. Nakamura, H. Hirai, and T. Kurokawa. 1998. Modulation of osteoclast function by adenovirus vector-induced epidermal growth factor receptor. *J. Bone Miner Res*. 13:1714–1720.
Tezuka, K., T. Sato, H. Kamioka, P.J. Nijweide, K. Tanaka, T. Matsuo, M. Ohta, N. Kurihara, Y. Hakeda, and M. Kumegawa. 1992. Identification of osteopontin in isolated rabbit osteoclasts. *Biochem. Biophys. Res. Commun*. 186:911–917.
Traenckner, E.B., H.L. Pahl, T. Henkel, K.N. Schmidt, S. Wilk, and P.A. Baeuerle. 1995. Phosphorylation of human IκB-α on serines 32 and 36 controls IκB-α proteolysis and NF-κB activation in response to diverse stimuli. *EMBO (Eur. Mol. Biol. Organ.) J*. 14:2876–2883.
Van Aelst, L., M. Barr, S. Marcus, A. Polverino, and M. Wigler. 1993. Complex formation between RAS and RAF and other protein kinases. *Proc. Natl. Acad. Sci. USA*. 90:6213–6217.
Van Aelst, L., M.A. White, and M.H. Wigler. 1994. Ras partners. *Cold Spring Harb. Symp. Quant. Biol*. 59:181–186.
Vojtek, A.B., S.M. Hollenberg, and J.A. Cooper. 1993. Mammalian Ras interacts directly with the serine/threonine kinase Raf. *Cell*. 74:205–214.
Whitmarsh, A.J., and R.J. Davis. 1996. Transcription factor AP-1 regulation by mitogen-activated protein kinase signal transduction pathways. *J. Mol. Med*. 74:589–607.